What does not kill a tumour may make it stronger: *in silico* Insights on Chemotherapeutic Drug Resistance

Sara Hamis[1,2], Perumal Nithiarasu[3], Gibin G Powathil[1,2]

[1] Department of Mathematics, College of Science, Swansea University, Swansea, SA2 8PP, United Kingdom.
[2] Computational Foundry, Swansea University, Swansea, SA2 8PP, United Kingdom.
[3]Zienkiewicz Centre for Computational Engineering, Swansea University, Swansea SA1 8EN, United Kingdom.

Abstract

Tumour recurrence post chemotherapy is an established clinical problem and many cancer types are often observed to be increasingly drug resistant subsequent to chemotherapy treatments. Drug resistance in cancer is a multipart phenomenon which can be derived from several origins and in many cases it has been observed that cancer cells have the ability to possess, acquire and communicate drug resistant traits.

Here, we present an *in silico* framework that can simulate multiple types of drug resistance and study their role in chemotherapeutic treatment. This framework is based on a hybrid multiscale mathematical model. We investigate drug response in cancer cell populations hosting various types of drug resistant phenotypes, arising from inheritance or mutations that are spontaneous, drug-induced or communicated via exosomes. Our study shows that drug response in cancer cell populations is crucially influenced by the drug resistant phenotypes amongst the cells. This indicates that the effect of chemotherapy, and by extension optimal chemotherapy administration, is heavily dependent not only on the existence of drug resistance, but also the type of drug resistance.

Keywords

cancer, mathematical oncology, drug response, multiscale model, cellular automaton

1 Introduction

Chemotherapy is one of the major anticancer therapies, it is widely used both by itself and as part of multimodality treatment strategies. In most cases chemotherapy is effective, however the existence, or the development, of chemotherapeutic drug resistance in tumours continues to be a major problem in chemotherapeutic treatments, often leading to tumour recurrence post treatment [13, 24, 1, 29, 31, 47, 17]. Clinical and experimental observations suggest that cancers are often increasingly drug resistant subsequent to chemotherapy exposure [44, 47] and moreover cancer cells have the ability to posses, acquire and communicate drug resistant traits, enabling them to survive in the presence of chemotherapeutic drugs [24]. The existence of drug resistant phenotypes in cancer cell populations significantly impacts the efficacy and successfulness of chemotherapy [12, 57, 52].

The emergence of drug resistant cancer cells in tumours results in multiple subpopulations comprising drug sensitive (S) and drug resistant (DR) cells [12]. Furthermore cancer cell populations evolve according to Darwinian principles [53], consequently DR subpopulations may reach significant proportions in tumours despite initially accounting only for a small fraction of the cell population [24]. S and DR

subpopulations that coexist compete for resources such as space and nutrients [28, 53], this competition affects intratumoural heterogeneity. In cases where tumour eradication is implausible, chronic control treatments are proposed in which tumours are continuously managed and prohibited from reaching lethal proportions [18, 28, 24], long-term chemotherapy treatments are however linked to high frequency drug resistance [49, 30]. Since DR subpopulations are more fit than S subpopulations to survive in the presence of drugs, repeated or prolonged chemotherapy administration may amplify this fitness differentiation. Indeed Duan et al. [12] performed *in vitro* and *in vivo* experiments, they concluded that in absence of drugs, sensitive were more fit than drug resistant cells. Conversely, in presence of drugs the DR subpopulation dominated as the S subpopulation reduced [12]. Thus drug resistant cells may thrive in presence of drugs, and a large DR subpopulation may result in disease recurrence post chemotherapy [50]. Ensuring that the DR subpopulation does not dominate the S subpopulation is of importance as such an outcome would render the tumour uncontrollable by chemotherapy [28]. This suggests that deliberately maintaining a subpopulation of S cells may constitute a strategic countermeasure in tumour control schemes [34]. Duan et al. investigated the plausibility of this proposed strategy *in vivo* by comparing two cell populations exposed to chemotherapeutic drugs [12]. One of these cell populations comprised drug resistant cells only, and the other one contained a combination of both drug resistant and sensitive cells. Their study showed that the latter, combined, cell population was controllable by chemotherapy for a longer time period than the former, drug resistant, cell population [12].

Drug resistance is a multipart phenomenon which can be derived from several origins, in fact a cancer cell or tumour may express drug resistance in various ways [48, 24, 34]. Drug resistance may arise due to micro-environmental or intrinsic cell factors [14] and cells can acquire drug resistance by for example amplifying drug target molecules, activating DNA-repair, inducing drug transporters or altering their drug metabolism [48]. Phenotypical variations in cells, such as drug resistance, can be inherited or acquired and further, cells may be resistant to one specific drug or to multiple drugs, the latter phenomenon is known as multidrug resistance (MDR) [53, 30, 24, 22]. Early work performed by Luria and Delbrück on bacteria indicated that virus resistant mutations occur independently of the virus itself, thus indicating the existence of primary drug resistance [26]. These findings have since been adapted to oncology [13, 24], and primary drug resistance, that is drug resistance that occurs independently of the drug presence, is an accepted phenomenon arising from cell mutations. However, drug presence has been demonstrated to speed up the development of DR subpopulations [55] and cancer cells may acquire drug resistance by altering their genetic or epigenetic structure in order to evade drug effects [13]. Such alterations are induced by drug presence and may include dislodging drug receptors or overexpressing and modifying target molecules [13]. Typical chemotherapy drugs target cells in active cell cycle phases, thus quiescent cells parry drug effects [29] and similarly slow-cycling cells are intrinsically more drug resistant than fast cycling cells [50, 9]. Slow-cycling cells have been linked to cancer stem cell-like (CSC-like) cells [29], they are important drivers for tumours as they are more likely to evade drug effects and also may serve as reserve stem cells [50, 9]. CSC-like cells have been depicted to display various traits including being slow-cycling, migratory and non-adhesive [1]. Rizzo et al. [44] demonstrated *in vivo* in mouse tails that the subpopulation of CSC-like cells indeed benefits from drug presence. Thus slow-cycling cells have been identified to reinforce tumours, hence to eradicate cancers containing slow-cycling cells it is crucial to target both slow-cycling and fast-cycling cells [9]. Intracellular communication is vital for multicellular organisms and cells may communicate with each other using chemical signalling, direct physical contact or, as discussed here, sending and receiving exosomes [49, 59]. Out of these listed information mediators, exosomes are of particular interest as they are detectable, cell type-specific and able to travel long distances [49, 59]. This implies that they could potentially constitute therapeutic targets or biomarkers and thus be used to impede or signal cancer [49, 59]. Exosomes constitute subcellular "molecule-parcels" that cells may utilise to dispose of non-essential materials [59], however perhaps more interestingly, they facilitate long-distance intercellular communication by transporting information from sender cells to re-

cipient cells [49]. These molecule-parcels contain biomolecules such as proteins, mRNA and DNA which may provide recipient cells with information that can be used to alter phenotypical attributes, in order to increase fitness [59]. Exosomes are a type of extracellular vesicle (EV) [7] and recent studies have identified EVs as key players in cancer development as they can influence tumour growth and metastasis by communicating oncogenic information [59]. EVs have also been assumed to be a part of the process that converts non-malicious cells into cancerous, and of optimising the balance between CSCs and non-CSCs [59]. Thus in response to chemotherapeutic drugs, cancer cells may not only develop individual drug resistance, but furthermore they may render other cells drug resistant by secreting EVs to communicate and share drug resistant traits [7].

Mathematical models of tumour growth and treatment response may further cancer research by contributing insight into tumour dynamics, elucidating and validating clinically and experimentally recognised phenomena and guiding *in vitro* and *in vivo* experiments [18, 28, 24, 52, 53]. Further, in silico experiments have the advantage of cheaply being able to reproduce biological systems that span long time periods faster than real-time [53]. Various such mathematical models of tumour growth, treatment response and drug resistance have previously been proposed [36, 25, 33, 41, 24, 46, 6, 51]. Roose et al. presented a comprehensive review of models of avascular tumour growth [46] and Lavi et al. compiled an extensive report discussing previous work on mathematical models of drug resistance in cancer [24]. Monro et al. [28] presented a continuum model in which the tumour growth follows Gompertzian dynamics and drug resistant mutations occur proportionately to the tumour growth rate, in accordance with Luria Delbrück models. They concluded that increased drug administration may in fact reduce the survival length of a patient. Sun et al. [52] investigated therapy-induced drug resistance using a set of stochastic differential equations, they highlighted micro-environmental contributions to drug resistance. Powathil et al. [41] used the Compucell3D framework to investigate two coexisting subpopulations, specifically one fast-cycling and one slow-cycling, in the presence of drugs to demonstrate the intrinsic drug resistance of slow-cycling cells. There currently exists a number of hybrid discrete-continuum mathematical models that account for the multiscale nature of cancer, these models can be used to study tumour behaviour in response to multimodality treatment schemes [21, 35, 4, 15, 43, 3]. Likewise several modelling attempts have been made to address the multiscale aspects of cell growth by incorporating details such as vascular dynamics, oxygen transport, hypoxia, cell division and other intracellular features in order to study tumour dynamics and treatment response [32, 27, 37, 58]. A review of multiscale cancer models is available in the paper by Deisboeck et al. [10]. Recently, Powathil et al. [39, 20, 38] developed a hybrid multiscale cellular automaton, integrating cell cycle dynamics and oxygen distribution to study cell cycle-based chemotherapy delivery in combination with radiation therapy.

In the present *in silico* study, we propose a hybrid multiscale mathematical model that incorporates multiple types of drug resistance.*in silico* experiments are performed in order to study chemotherapeutic drug response in heterogenous cancer cell populations hosting various types of drug resistant phenotypes pre, peri and post chemotherapy.

2 Model and *in silico* Framework

Following previous work by Powathil et al. [39], tumour growth and drug dynamics are modelled with a cellular automaton (CA). An overview of the relevant multiscale hybrid modelling techniques can be found in a later paper by Powathil et al. [40]. In this study, we expand on this model to incorporate multiple types of mechanisms that elicit drug resistance in cancer cells. The CA extends in two spatial dimensions, specifically a 100 by 100 square grid is utilised to simulate a physical tissue slab of $(2\text{ mm})^2$. This agrees with biological dimensions and each grid point is occupied by a cancer cell, a blood vessel cross section or extracellular matrix [39]. At the start of the *in silico* experiment one initial cancer cell

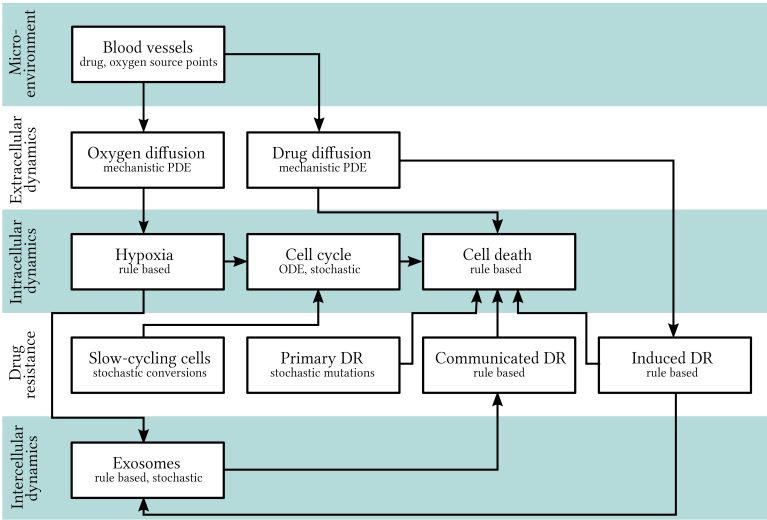

Figure 1: A schematic representation of the multiscale hybrid mathematical model. The model integrates extracellular, intracellular and intercellular dynamics. Various categories of drug resistance regarded on a cellular resolution are incorporated, these categories are listed in Table 1.

is planted at the centre of the grid, over time this cell divides to give rise to a population of cancer cells and eventually chemotherapeutic drugs are applied to the system. Blood vessels are non-equidistantly scattered across the grid, they are assumed stationary and perpendicular to the two-dimensional tissue slab. Thus blood vessel cross sections live on the grid, where they act as source points for oxygen and drugs. As shown in the model schematics in Figure 1, our model is multiscale and incorporates a non-uniform micro-environment, extracellular dynamics, intracellular dynamics, intercellular dynamics and various categories of drug resistance regarded on a cellular resolution. This is a hybrid CA model that uses mechanistic partial differential equations (PDEs), ordinary differential equations (ODEs) extracted from a regulatory molecular network, as well as stochasticity and phenomenological rules formulated by observations from biological experiments and clinical remarks.

2.1 Intratumoural heterogeneity

Tumours are dynamic and should therefore be treated as such [48], they are also heterogeneous and may constitute multiple distinguishable subpopulations [48] [53]. Intratumoural heterogeneity has been observed to promote drug resistance [48, 52] and hinder successful tumour prediction, thus by extension this heterogeneity complicates intelligent chemotherapy administration [53]. A tumour can express intratumoural heterogeneity in various ways. For example nutrient concentrations, cell cycle dynamics and drug resistant traits may vary amongst cells in a tumour [52, 53]. Phenotypical attributes, such as drug resistant traits, may be acquired or inherited [53] and moreover stochasticity occurs naturally in biological processes. Hence various phenotypical subpopulations may arise in a cell population, even if the population originates from one single cell [48]. To effectively treat tumours one should thus account for intratumoural heterogeneity, including the potential uprising of drug resistant subpopulations [53]. Our model accounts for intratumoural heterogeneity on various scales, details are given in the following sections. On a cellular level, each cell has an individual cell cycle length and on an extracellular level, oxygen and drug concentrations vary across the grid and moreover the micro-environment is asymmetric as the blood vessels are non-equidistantly placed. Furthermore, when determining if a cell is drug resistant or not, each cell is here evaluated individually.

2.1.1 Intracellular dynamics

The cell cycle mechanism can be partitioned into four sequential main phases, namely the gap 1 (G1), synthesis (Syn), gap 2 (G2) and mitosis (M) phase. In the synthesis phase, the DNA duplicates and in the mitoses phase chromosome segregation and cell division occur [19]. Between these two phases a cell requires time to grow and double its protein and organelle mass in order to replicate its DNA and divide, such intermediate phases are dubbed the gap phases. If some conditions are unfavourable a cell may delay its reproduction progress by exiting the cell cycle to enter an inactive, quiescent phase (G0) [39]. In the model, cancer cells are categorised as being in either the G1 phase or in the collective Syn-G2-M phase of the cell cycle, alternatively cells can exit the cell cycle and enter the quiescent phase G0 [39]. The cell cycle of each individual cell is governed by a regulatory molecular network described by a system of ODEs (Equation 1) [39] in which the dependent variables are protein concentrations and cell mass ($mass$). The relevant proteins are namely the Cdk-cyclin B complex ($CycB$), the APC-Cdh1 complex ($Cdh1$), the p55cdc-APC complex in its total form ($p55cdc_T$) and active form ($p55cdc_A$), and finally the Plk1 protein in its active form ($Plk1$). The Cyclin B value is used as a marker to determine which state of the cell cycle that the cell is in, and by extension when cell division occurs as this happens when the cell exits Syn-G2-M phase to enter the G1 phase. When cell division occurs in the model, a daughter cell is placed on a grid point in the spherical neighbourhood of the parental cell. Grid points in lower order neighbourhoods are prioritised in this process, however up to third-level neighbourhoods are regarded. Each cell may divide until there is no unoccupied grid point on which to place a daughter cell, when this occurs a cell enters the quiescent phase G0. A cell may however re-enter the cell cycle if its neighbourhood is freed up and space is made available. Whilst in a quiescent phase cells are assumed to be drug resistant in our model, this is because classical chemotherapy drugs target molecules that are overexpressed in specific cell cycle phases, for example the drug cisplatin affects the G1 phase of the cell cycle [39, 56]. The ODE that regulates the cell cycle reads

$$\frac{d[CycB]}{dt} = k_1 - (k_2' + k_2''[Cdh1] + [p27/p21][HIF])[CycB], \tag{1a}$$

$$\frac{d[Cdh1]}{dt} = \frac{(k_3' + k_3''[p55cdc_A])(1 - [Cdh1])}{J_3 + 1 - [Cdh1]} - \frac{k_4[mass][CycB][Cdh1]}{J_4 + [Cdh1]}, \tag{1b}$$

$$\frac{d[p55cdc_T]}{dt} = k_5' + k_5'' \frac{([CycB][mass])^n}{J_5^n + ([CycB][mass])^n} - k_6[p55cdc_T], \tag{1c}$$

$$\frac{d[p55cdc_A]}{dt} = \frac{k_7[Plk1]([p55cdc_T] - [p55cdc_A])}{J_7 + [p55cdc_T] - [p55cdc_A]} - \frac{k_8[Mad][p55cdc_A]}{J_8 + [p55cdc_A]} - k_6[p55cdc_A], \tag{1d}$$

$$\frac{d[Plk1]}{dt} = k_9[mass][CycB](1 - [Plk1]) - k_{10}[Plk1], \tag{1e}$$

$$\frac{d[mass]}{dt} = \mu[mass](1 - \frac{[mass]}{m_*}), \tag{1f}$$

where the coefficient μ is individual to each cell and depicts cell growth rate, it takes a randomised value within an allowed range to account for heterogeneous cell cycle lengths amongst cells [39]. The variable $[HIF]$ corresponds to the hypoxia inducible transcription factor-1 (HIF-1) pathway, in the model this factor is activated if the cell is classified as hypoxic [39] so that $[HIF] = 1$ in hypoxic cells and $[HIF] = 0$ in normoxic and hyperoxic cells. Oxygen distribution, and by extension hypoxia, is governed by an extracellular PDE, hence extracellular and intracellular dynamics are here integrated. Parameters are listed in the supplementary material.

2.1.2 Extracellular dynamics

Extracellular dynamics is modelled using mechanistic PDEs describing oxygen and drug distribution. Oxygen is continuously produced at each time step on the blood vessels cross sections from which it is distributed across the grid according to a diffusion-reaction equation (Equation 2) [39],

$$\frac{\partial K(x,t)}{\partial t} = \nabla \cdot (D_k(x,t)\nabla K(x,t)) + r_k(x,t)m(x) - \phi_k K(x,t)cell(x,t), \tag{2}$$

where $K(x,t)$ denotes oxygen concentration in location x at time t, $D_k(x,t)$ is the oxygen diffusion coefficient, $r_k(x,t)$ is the oxygen production rate and ϕ_k is the oxygen consumption rate. The variables $m(x)$ and $cell(x,t)$ are binary so that $m(x) = 1$ if there is a blood vessel in location x and $m(x) = 0$ otherwise. Likewise $cell(x,t) = 1$ if there is a cell in location x at time t and $cell(x,t) = 0$ otherwise. No-flux boundary conditions are applied, such boundary conditions coupled with the oxygen production at each time step will cause the total oxygen in the system to fluctuate over time and thus the hypoxic threshold takes a relative value. Specifically a grid point is defined to be hypoxic if it has a oxygen concentration drug less than 0.1, where an oxygen concentration of 1 is normalised at the grid point with the highest oxygen concentration on the grid. Oxygen diffuses slower over grid points occupied by cancer cells than elsewhere and sufficiently high oxygen concentrations promote rapid cell proliferation, whilst hypoxia hinders cell cycle advancement. These hypoxic effects are incorporated in the model via the $[HIF]$ parameter occurring in Equation 1 [39]. Chemotherapy drugs are similarly administered via blood vessel cross sections, however drugs are instantaneously produced at one single time step per drug administration. Drugs diffuse according to Equation 3,

$$\frac{\partial \mathscr{C}(x,t)}{\partial t} = \nabla \cdot (D_c(x)\nabla \mathscr{C}(x,t)) + r_c(x)m(x) - \phi_c \mathscr{C}(x,t)cell(x,t) - \eta_c \mathscr{C}(x,t), \tag{3}$$

using no-flux boundary conditions. Here $\mathscr{C}(x,t)$ denotes drug concentration in location x at time t, $D_c(x,t)$ is the drug diffusion coefficient, $r_c(x,t)$ is the drug production rate, ϕ_c is the drug consumption rate and η_c is the drug decay rate. Chemotherapy drugs diffuse faster across extracellular matrix than inside the tumour [39]. Parameters occurring in the PDEs are listed in the supplementary material.

2.2 Drug resistance

In this study, drug resistance is regarded on a cellular resolution, thus subcellular mechanics are simplified and drug resistance is categorised into cellular-level categories as illustrated in Figure 2. In the model drug resistance is firstly categorised as being either explicit or implicit. Explicit drug resistance occurs when a cell possesses any subcellular trait that directly protects it from drug effects. Conversely, a cell displays implicit drug resistance when it is shielded from drug impact due to some indirect reason such as being slow-cycling or spatially located in a region of low drug concentration. Drug resistant traits can be induced or inherited [23, 45] and also, cells may perform phenotypical alterations in response to intercellular interactions [48]. Therefore we here categorise drug resistance as being induced, primary or communicated. Induced drug resistance is activated in cells as a defensive response to drug presence whilst primary drug resistance is caused by cell mutations occurring independently of drugs [23, 45]. Cancer cells in which drug resistance has been induced may communicate and spread their resistant traits to other cancer cells via intracellular communication (ICC) in an effort to secure species survival [49, 59, 7]. Using hybrid modelling, the various categories of drug resistance are here modelled in different ways in order to easily reproduce biological phenomena in a way that is consistent with available clinical and experimental observations and data. In our model, drug resistance obeys rules formulated from previous findings from *in vitro* and *in vivo* results. We also incorporate stochastic methods, as stochasticity occurs naturally in biological processes and may generate different cell phenotypes [48]. For all categories of drug resistance, we are assuming that once a cell has established drug resistant traits, its offspring will inherit

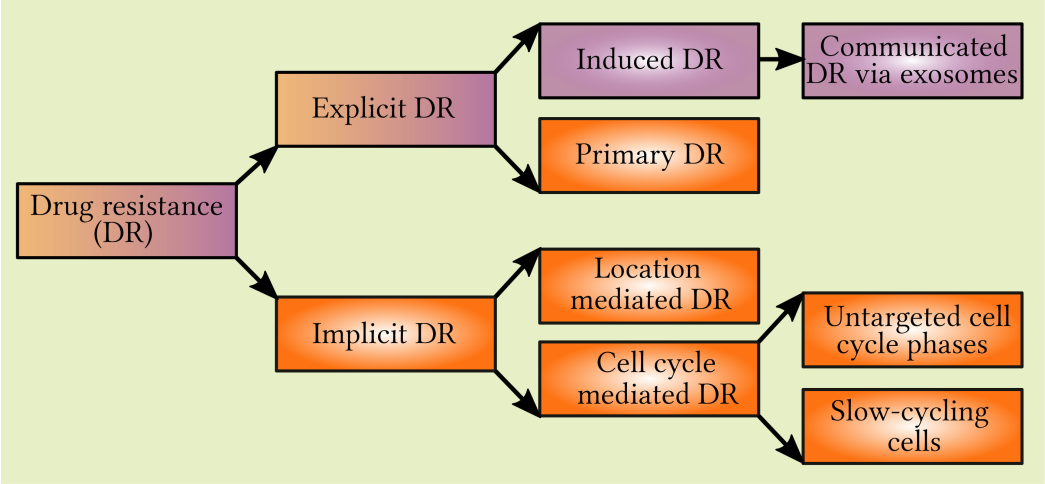

Figure 2: Classification of drug resistance categories occurring in the model. Drug resistance may be independent of drug presence (orange labels), induced by drug presence (purple labels), or either (orange and purple labels).

those traits. This is in accordance with evolutionary Darwinian principles, as DR subpopulations are more fit to survive in drug presence than are S subpopulations [16]. Furthermore, the micro-environment influences drug transport across the tumour, impeded drug delivery by poor diffusion is indeed one of the primary reasons for treatment failure [24]. Thus drug efficacy and cytotoxic cell death is affected by the micro-environment, since drugs may not reach target cells. This may occur if the drug diffusion is impeded by dense population regions, or if the target cells are spatially located far away from drug source points, here blood vessels. To study how a heterogeneous micro-environment impacts drug resistance and drug response, blood vessels are non-equidistantly located across the *in silico* domain. Moreover, the speed of molecules such as oxygen, drugs and exosomes, depends on the medium that the molecules in question are traversing [39, 49]. This section provides information regarding the modelling of various drug resistant categories. Numerical values of the parameters introduced in this section are listed in the supplementary material, along with schematic representations of algorithms used in the model and a sensitivity analysis which demonstrates that our results are robust in regards to these parameters. Thus our qualitative findings, concerning drug response in cancer cell populations hosting various types of drug resistance, hold for variations of our chosen parameters.

2.2.1 Primary drug resistance

Cells display primary drug resistance independently of drug presence, thus primary drug resistance may precede chemotherapy [26, 45, 24]. The *in silico* setup in our study is analogous to Luria and Delbrück's [26] *in vitro* experiment, however here bacteria and virus have been exchanged for cancer cells and chemotherapy drugs respectively. Luria and Delbrück [26] stated that there was a probability per unit time that a sensitive cell would mutate into a drug resistant phenotype. Thus in accordance with Luria and Delbrück models [26], primary explicit drug resistance is here modelled by stochastic cell mutations. More specifically the chance of mutation is given by the mutation rate α_{pri}, which corresponds to the probability of mutation per cell cycle. The parameter α_{pri} is assumed to be small, so that drug resistant mutations are rare and moreover the probability that a mutated cell will revert back to a sensitive state is negligible and set to zero [26]. Hence in our model each daughter cell that is produced has a chance α_{pri} of being explicitly drug resistance before being placed on the grid.

2.2.2 Induced drug resistance

Drug presence has been demonstrated to speed up the development of DR subpopulations in cancers [55] and multiple studies have shown that cancer cells display altered epigenetic features following chemotherapy [23]. Cancer cells may become drug resistant after exposure to chemotherapy, the underlying cause of such induced drug resistance is assumed multifactorial [45]. Factors that may contribute to induced drug resistance include decreased apoptotic response, increased DNA-repair post drug-mediated damage, cell cycle alterations and reduced drug accumulation [45]. These factors may work concurrently and jointly towards establishing drug resistance in cells [45]. In clinics cancers are usually treated with combination therapies which makes it difficult to deduce rigorous information regarding how induced drug resistance is developed in cells as a response to one particular drug [54]. Due to this multifactorial nature of induced drug resistance, that involves various subcellular alterations occurring in response to drug presence in the micro-environment, in the model a cell obtains induced implicit drug resistance once it has been exposed to a high enough drug concentration for a long enough amount of time. Thus if a cell has experienced a minimum drug concentration χ_{ind} for τ time units, drug resistance is induced in the cell.

2.2.3 Communicated drug resistance via exosomes

Srinivasan et al. [49] investigated exosome kinetics in lymphatic flow *in vitro* and *in vivo* using near infrared imaging. In the *in vitro* study, they found that planted exosomes from the HEY cell line, being spherical with a diameter of around 70 nm, travelled more effectively than size and density matched beads across lymphatic endothelial cells (LECs). This indicates that exosomes travel purposefully as opposed to randomly. Srinivasan et al. [49] reported a propagation speed in the order of 0.2 μm for exosomes across LECs, twice the speed of exosomes across areas with no cells. Exosomes were observed to move rapidly *in vivo*, indeed they travelled 10 cm in a mouse tail within 2 minutes [49]. Studies also show that there is a correlation between the micro-environment and exosome activity, as exosome secretion and uptake is promoted in low-pH regions [59]. Further, hypoxic regions are associated with drug resistance [2] which is partly explained by elevated exosome secretion in such regions [7]. Here, exosomes are modelled using phenomenological rules formulated from experimental observations, incorporating stochasticity. Exosomes are modelled as discrete "molecule parcels". Once per cell cycle each cell that has acquired induced drug resistance has a chance α_{ex} of producing and secreting such a molecule parcel which is sent off in a random direction. The first sensitive cell that the exosome hits is dubbed the recipient cell, upon receiving the exosome the recipient consumes the parcel to gain drug resistance. Exosome production and uptake time are incorporated in the travel time and thus modelled as instant, using data from Srinivasan et al. [49] we choose a propagation speed of 0.2 μm per second which is equivalent to 1 grid point (20 μm) per 100 s when travelling across cells, and half of this speed when travelling across extracellular matrix. The chance of exosome production α_{ex} is significantly higher in hypoxic regions to account for the increased exosome activity in such regions [7].

2.2.4 Cell cycle mediated drug resistance by slow-cycling cells

Slow-cycling cells are distinguishable *in vitro* [9] and Srinivasan et al. [50] demonstrated that fast and slow-cycling cells may coexist in a tumour. Chemotherapeutic drugs, such as cisplatin, attack only cells in a certain phase of the cell cycle by targeting proteins overexpressed in the corresponding phase, leaving other cells unaffected [39, 56]. Since the half-life times of common chemotherapy drugs are significantly shorter than the average cell cycle length of standard eukaryotic cells [39], slow-cycling cells are implicitly more resistant to chemotherapy as they are likely to evade drug impact whilst being in a prolonged untargeted cell cycle phase. Consequently, if there exists a subpopulation of slow-cycling cells in a tumour, this subpopulation is more likely to survive chemotherapy and proliferate post treatment, despite having a slower production rate. Such a slow-cycling subpopulation may comprise CSC-like cells, as slow-cycling cells have been linked to cancer stem cells [29]. Previous research indicates that cancer

Label	Drug Resistance Category
a	No drug resistance (No DR)
b	Primary drug resistance (Primary DR)
c	Induced drug resistance (Induced DR)
d	Induced and, via exosomes, communicated drug resistance (ICC DR)
e	Cell cycle mediated drug resistance by spontaneous conversion to slow-cycling cells (SC DR)

Table 1: The labelling of drug resistance categories occurring in the model.

cells may obtain stem-cell like traits [11], in fact non-stem cancer cells may convert to CSC-like cells spontaneously, as demonstrated *in vivo* by Chaffer et al. [8]. Slow-cycling cells are multidrug resistant as they are resistant to any drug that targets only a subset of cell cycle phases. In the model we assume that slow-cycling conversion occurs spontaneously, independently of drug presence. More specifically once per cell cycle there is a chance α_{SC} that a sensitive, fast-cycling cell will spontaneously convert into a slow-cycling state. Here slow-cycling cells are assumed to have a cell cycle length that is twice as long as a sensitive cell [41]. The chance of conversion from a slow-cycling, implicitly drug resistant state to a fast-cycling state is assumed negligible in accordance with previously discussed Luria Delbrück models [26] and Darwinian principles and thus set to zero.

2.3 Implementation

The CA is implemented in C/C++ using a high performance computational framework. Ordinary differential equations are solved using a fourth order Runge-Kutta method and partial differential equations are solved using explicit finite difference schemes. Prior to commencing the *in silico* experiment, the micro-environment is implemented and thus blood vessel cross sections are scattered in a non-equidistant fashion across the grid, this is in order to emphasise and study the effects of oxygen and drug heterogeneity. One initial cancer cell is then planted at the centre of the grid, from this originating cell the cancer cell population will grow. Tumour growth is simulated over 700 hours using a time step size $\Delta t = 10^{-4}$ hours, we concluded that 700 hours is a sufficiently long simulation time to study the drug resistance and drug response in our system. Cisplatin, a chemotherapy drug that attacks G1 cells, is administered in two instances at 500 and 600 hours. The drug dosage is (1) 1C, (2) 2C, (3) 4C or (4) 8C, where the unit C is normalised so that, in the absence of drug resistant phenotypes amongst the cells, 1 C kills half of the population shortly after the first drug administration at 500 hours. For this fixed chemotherapy schedule we vary the administered drug dosage and compute the size of sensitive and drug resistant cell subpopulations pre, peri, and post chemotherapy. Cell-maps are produced to display cell population topology over time, these cell-maps are visualised in ParaView [5]. We perform five different *in silico* experiments, corresponding to five different categories of drug resistance namely (a) to (e) listed in Table 1. Each experiment is performed 100 times, subsequently average values and standard deviations are computed. A sensitivity analysis is performed in order to confirm that our results are robust in regards to small parameter variations. This sensitivity analysis it available in the supplementary material.

3 Results and Discussion

3.1 Results

In absence of chemotherapeutic drugs, the growth of the DR subpopulation in our *in silico* experiment is proportional to the growth of the S subpopulation, as demonstrated by the graphs in Figure 3. This is in accordance with previous mathematical models and experimental results [28, 26, 24].

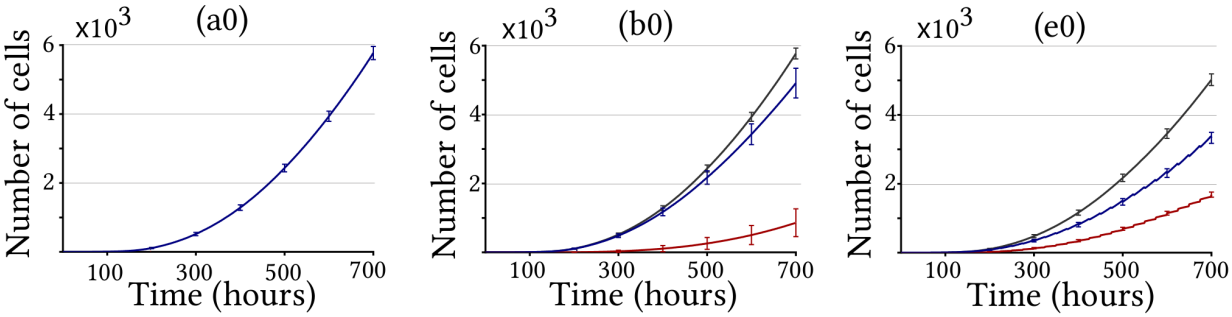

Figure 3: Growth of the cancer cell population over time in drug absence, showing total population (black graph), drug sensitive subpopulation (blue graph) and drug resistant subpopulation (red graph) incorporating drug resistance categories (a0) No DR, (b0) Primary DR and (e0) SC DR. Cases (c0) Induced DR and (d0) ICC DR are omitted since they produce the same results as (a0) in drug absence. Each graph shows the average number of cells based on 100 simulations, the standard deviation is demonstrated with error bars.

3.1.1 No drug resistance

Once chemotherapy is applied to our *in silico* setup, the cancer cell population decreases in response to drugs. This is especially clear when no drug resistant phenotypes exist, the cancer cell population then rapidly reduces after drug administration. However population growth quickly resumes, and the size of such populations eventually reaches, and surpasses, the pre-chemotherapy population size. This is evident in graphs (a1) through to (a4) in Figure 4, and especially clear for high chemotherapy dosages where the size of the cell population cycles between being large immediately before drug administration and being small directly after drug administration. Rottenberg and Borst [47] demonstrated similar cyclic behaviour in mouse tails *in vivo*. Increasing the drug dosage trivially kills more cancer cells, however tumour topology and spatial heterogeneity significantly affects drug transport. Moreover, due to intratumoural heterogeneity in regards to the cell cycle, some cells will be shielded from the drug simply by being in an untargeted cell cycle phase. This multiscale heterogeneity affects the relationship between drug dosage and drug efficacy, where drug efficacy here corresponds to the number of cells killed by the drug. Graphs (a1) to (a4) in Figure 4 demonstrate the poor scaling between drug dosage and drug efficacy. Further, here we define the scaling efficiency by

$$\epsilon_i = \frac{k_i}{k_1 \cdot N_i},$$

where k_i denotes the number of cells killed in experiment i and N_i denotes the dosage used in experiment i. Thus here, $i = 1, 2, 3, 4$ and respectively $N_i = 1, 2, 4, 8$ C. If the relationship between drug dosage and drug efficacy was linear, doubling the dosage would mean doubling the number of cancer cells killed. In such an ideal case it would hold that $\epsilon_i = 1 \, \forall i$, however this is not the case, as illustrated in Figure 5 which shows the scaling efficiency for the first drug administration at 500 hours. Hence in a clinical setting, the harm that may follow increased toxicity from higher drug dosages may not be worth the modest increase in killed cancer cells. The cell-maps in Figure 6 further highlight how the spatial heterogeneity affects drug transportation and consequently where the drug concentrations are high enough for cell kills to occur.

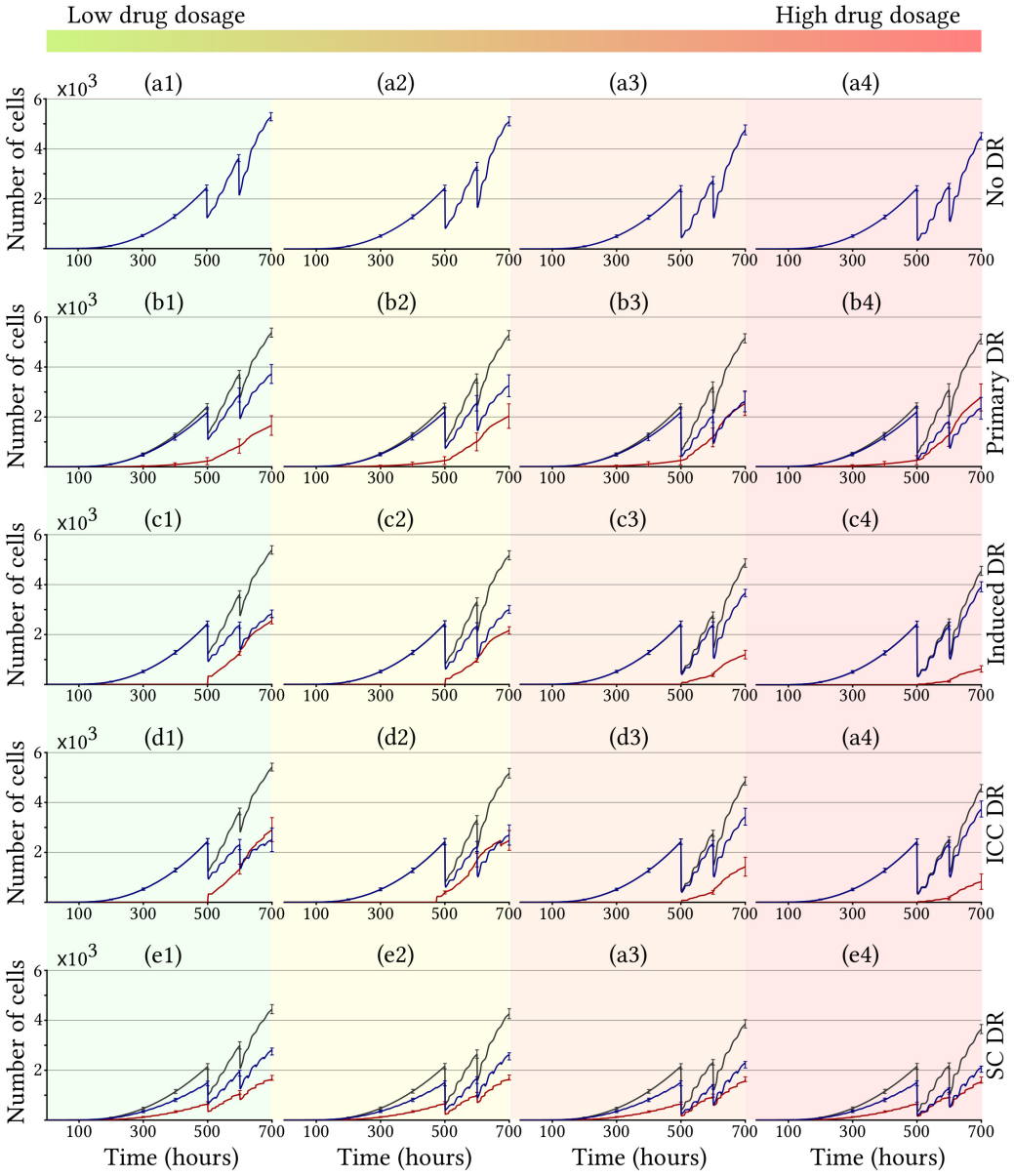

Figure 4: Growth of the cancer cell population over time when drugs are applied at 500 and 600 hours, showing total population (black graph), drug sensitive subpopulation (blue graph) and drug resistant subpopulation (red graph) for drug resistance categories (a0) No DR, (b0) Primary DR, (c0) Induced DR, (d0) ICC DR and (e0) SC DR. Each row in the figure corresponds to a category of drug resistance (a) to (e), whilst each column corresponds do a specific drug dosage varying from low (leftmost column) to high (rightmost column), namely (1) 1C, (2) 2C, (3) 4C and (4) 8C. Each graph shows the average number of cells based on 100 simulations, the standard deviation is demonstrated with error bars.

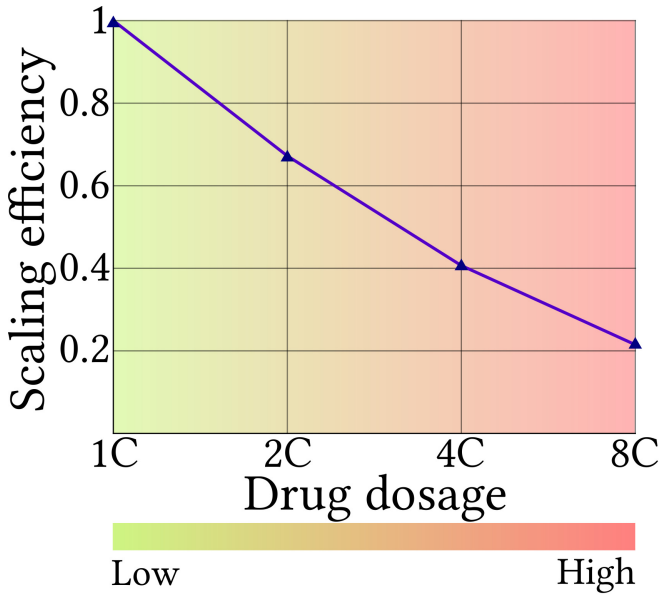

Figure 5: The scaling efficiency, demonstrating the relationship between drug dosage and drug efficacy in terms of number of killed cancer cells. This is for the first drug administration at 500 hours for experiments (a1) to (a4), where no drug resistant phenotypes are present. Results are based on average values for 100 tests.

3.1.2 Primary drug resistance

When a cancer cell population expresses primary drug resistance, two subpopulations, comprising sensitive and drug resistant cells, already coexist prior to chemotherapy. Once administered, chemotherapy eliminates cells belonging to the S subpopulation whilst leaving the DR subpopulation unharmed. Hence increasing the drug dosage, and consequently killing more sensitive cells, enables the DR subpopulation to flourish as it gains access to more resources such as space and oxygen. Graphs (b1) through to (b4) in Figure 4 show that such DR subpopulations indeed benefit from high drug environments. Over all, our results show that chemotherapeutic treatments yield poor results if there exists a subpopulation of drug resistant cells prior to commencing treatment, this supports clinical observations depicting that primary drug resistance gravely reduces the successfulness of chemotherapy and influences the choice of treatment regime [13]. In our experiment, primary DR subpopulations grows outwards in radial strands pre chemotherapy, as illustrated in cell-maps (b1) and (b4) in Figure 6. This geometry is explained by the model, in which primary drug resistant mutations occur at cell division, prior to placing the cell on the grid. Moreover drug resistant cells produce drug resistant offspring, thus radial strands are formed as the cancer cell population grows. This DR subpopulation will spread from these strands, which consequently will widen, post drug administration. On the other hand, subpopulation S will spread from regions containing sensitive cells that survived drug effect. Such sensitive survivor cells are clustered in regions of low drug concentrations, typically located far away from blood vessels and enclosed by other cancer cells, as drugs travel more slowly over dense population regions.

3.1.3 Induced drug resistance

For simulations incorporating induced drug resistance, the DR subpopulation arises post chemotherapy. Here drugs diffuse more slowly over cancer cells than over extracellular matrix. Therefore, once the

initial effect of chemotherapy has eliminated the majority of the sensitive cancer cells, and the tumour has disintegrated into clusters of surviving cancer cells, drug resistant cells are typically located on boundaries between cancer cells and extracellular matrix, as illustrated in cell-maps (c1) and (c4) in Figure 7. On these boundaries drug resistance is induced since the cells are exposed to high, but non-lethal, drug concentrations for a sufficiently long time. From these points of origin the DR subpopulation will spread. By increasing the amount of chemotherapy, the cells that are exposed to this intermediate, high but non-lethal, drug concentration is reduced. Hence higher chemotherapy dosages do not only kill more cells overall, but reduces the amount of drug resistant phenotypes, as demonstrated by graphs (c1) to (c4) in Figure 4. This result applies to a cancer cell population in a confined space.

3.1.4 Communicated drug resistance via exosomes

The effect of ICC is demonstrated by comparing experiment (c) Induced drug resistance, to experiment (d) Induced and, via exosomes, communicated drug resistance. This can be done by regarding graphs (c1) to (c4) and (d1) to (d4) in Figure 4 and cell-maps (c1), (c4), (d1), (d4) in Figure 7. These figures show that the communicative exosome component amplifies the effect of induced drug resistance alone. The number of oncogenic exosomes produced increases with the number of drug resistant cells. In low to moderate drug environments, many exosomes are thus produced, as there exists many cells which have acquired induced DR in accordance with the results in Section 3.1.3. Conversely, in very high drug regimes fewer cells will survive to acquire induced drug resistance and consequently fewer oncogenic exosomes will be produced. Exosomes have been hypothesised as possible treatment targets, and our results indicate that reducing the exosome activity would aid the S subpopulation, as less cells would convert from sensitive to drug resistant. Here, hypoxic cells secrete more exosomes than do normoxic cells. This results highlights one of the benefits of targeting hypoxic tumour regions, as doing so may reduce exosome activity and by extension hinder communicated drug resistance.

3.1.5 Cell cycle mediated drug resistance by slow-cycling cells

Slow-cycling cells are more likely to evade drug effects, as shown in graphs (e1) to (e4) in Figure 4 where, after each drug attack, the DR slow-cycling subpopulation displays a higher survivor rate. High chemotherapy dosages increase this effect, and thus benefit the DR subpopulation. Since the conversion to slow-cycling cells is modelled as spontaneous, implicit drug resistance may precede chemotherapy. Furthermore this spontaneity means that at every cell cycle, each fast-cycling cell has the same chance α_{SC} of converting to a slow-cycling state. Thus pre chemotherapy the DR subpopulation will be point-wise scattered across the cell population, and post chemotherapy the DR subpopulation will spread from these source points, as illustrated in cell-maps (e1) and (e4) in Figure 7.

3.1.6 Cell-map topology

Each drug resistance category in our model corresponds to a typical cell-map topology and vice-versa, as shown in Figures 6 and 7. The location of the subpopulations S and DR depends on the category of drug resistance regarded, as does the location of regions with high cell-kill numbers. These cell-maps are useful for conveying spatial heterogeneity, which is of importance since intratumoural heterogeneity is known to heavily influence drug efficiency [39]. Any sensitive cell, or cell cluster, that is surrounded by a band of other cells will be partly shielded from drug effects, as drugs travel slowly over dense population regions. Further, any quiescent sensitive cell, or cell cluster, that is surrounded by a band of explicitly drug resistant cells is eternally safe from drug presence in our *in silico* setup. This is because such a sensitive cell, or cell cluster, will never meet the necessary condition to re-enter the cell cycle as this requires free neighbourhood space. Thus even sensitive cell may be protected from drug effect, this is an example of location mediated implicit drug resistance.

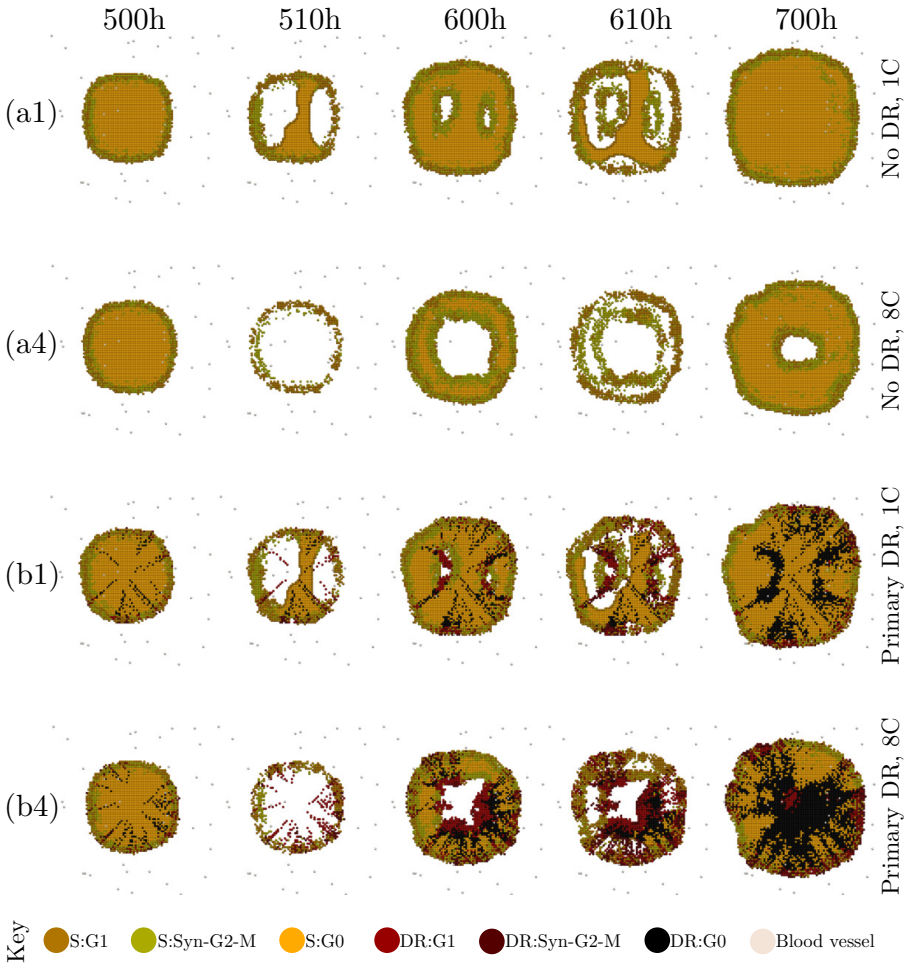

Figure 6: Cell-maps of the cancer cell populations at times 500 h (immediately before first drug dose), 510 h 600 h (immediately before second drug dose), 610 h and 700 h (end of simulation). Cases incorporating (a) No DR and (b) Primary DR are shown for drug dosages of (1) 1C and (4) 8C.

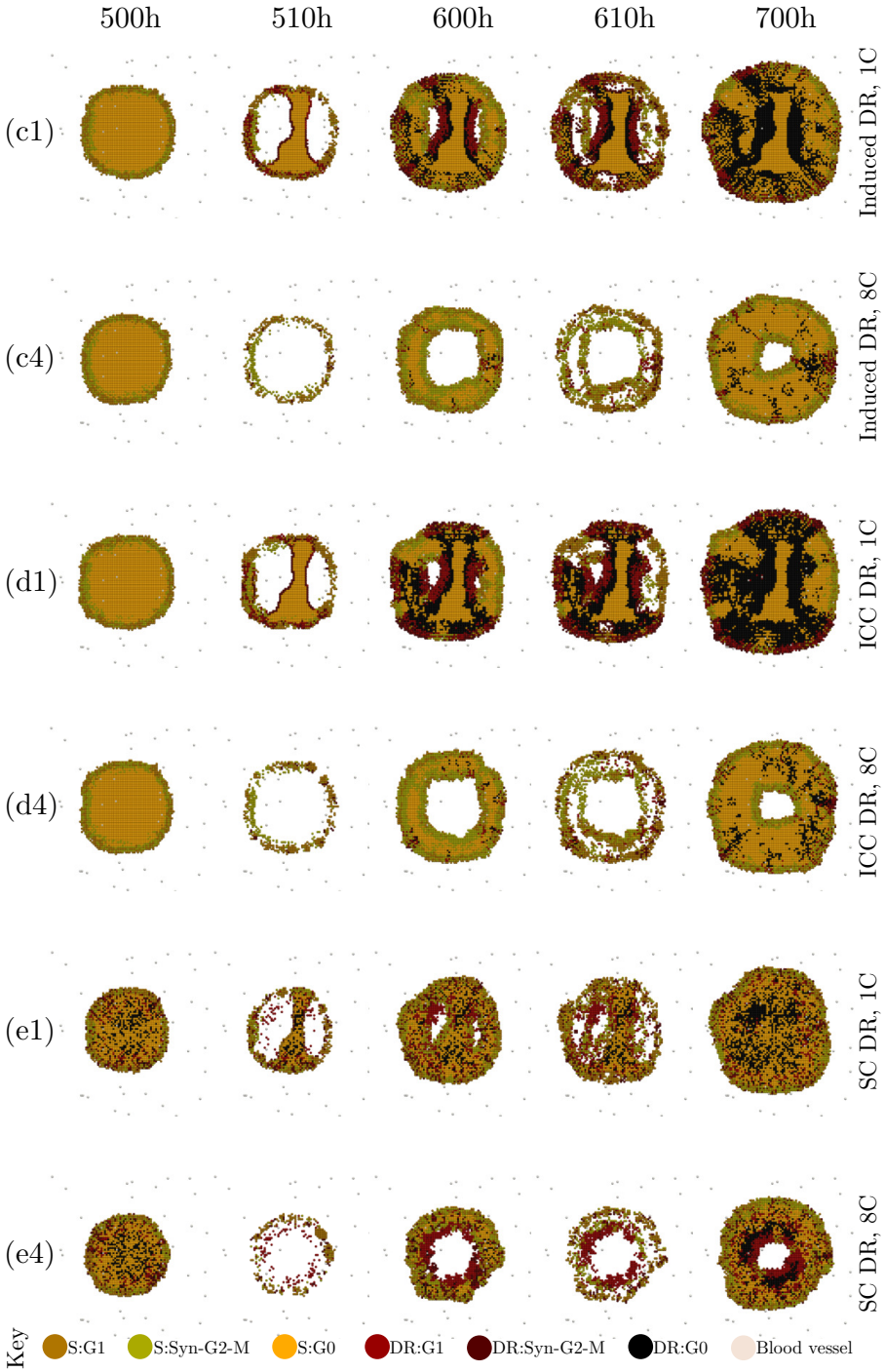

Figure 7: Cell-maps of the cancer cell populations at times 500 h (immediately before first drug dose), 510 h 600 h (immediately before second drug dose), 610 h and 700 h (end of simulation). Cases incorporating (c) Induced DR, (d) ICC DR and (e) SC DR are shown for drug dosages of (1) 1C and (4) 8C.

3.2 Discussion

Our study shows that drug response in cancer cell populations is crucially influenced by the drug resistant phenotypes amongst the cells. *in silico* we demonstrate that the effect of chemotherapy is heavily dependent not only on the mere existence of drug resistance, but also the type, or category, of drug resistance. Clinically this implies that optimal chemotherapy schedules and dosages depend on information regarding any drug resistant phenotypes hosted by a tumour. Indeed our results show that some types of drug resistant phenotypes thrive in low drug settings, whilst other flourish in high drug settings.

Before proceding to discuss optimal drug dosages, one must define what constitutes as "successful" chemotherapy. Is the aim perhaps to *(i)* reduce the cancer cell population as much and quickly as possible or to *(ii)* be able to control the tumour long-term using chemotherapy? Case *(i)* may be relevant when chemotherapy is used in combinations with other treatments, for example when neoadjuvant chemotherapy is used prior to radiation treatment or surgery. Conversely, Case *(ii)* may be applicable when chronic chemotherapeutic treatment strategies are used, as can be done when it is implausible to completely eliminate a tumour. In such cases it is vital to suppress any DR subpopulation in order to keep the tumour manageable by chemotherapy. For Case *(i)*, Figure 8 provides the data needed to discuss intelligent treatment strategy. This diagram trivially shows that high chemotherapy dosages are the most effective to rapidly eradicate cancer cells. However, what is not shown in our result, but is of clinical importance, is that high drug dosages are coupled with high toxicity which may be detrimental to patients. Moreover our results show that the efficiency between drug dosage and drug efficacy scales poorly, which is worth considering in a clinical setting. The increase in toxicity following from an increased drug dosage may not validate the outcome in terms of tumour reduction. In Case *(ii)* there is a balance, and sometimes a trade-off, between eliminating sensitive cells and aiding the drug resistant cells. Indeed killing of sensitive cells paves the way for any drug resistant phenotypes. Hence administering low chemotherapy dosages sometimes constitutes a wiser treatment strategy as it delays the uprising of a drug resistant subpopulation. Evolutionary theory and the interaction between S and DR subpopulations may play a role in designing intelligent treatment strategies. Figure 9 shows the ratio between S and DR subpopulations at different times. This diagram demonstrates that drug resistant phenotypes that arise independently of drug presence benefit from high drug dosages. However, *in silico*, the opposite is true here for drug-induced drug resistant phenotypes, which prosper in low drug conditions. Ideal chemotherapeutic tumour treatments would involve rapidly reducing tumour size whilst minimising drug resistance, thus meeting the goals of both Cases *(i)* and *(ii)*. However, our results indicate that when using chemotherapy only, there is a trade-off between tumour reduction and the suppressing of drug resistant phenotypes in some cases, thus the objectives of case *(i)* and *(ii)* may conflict.

4 Conclusion

Enhanced chemotherapeutic drug resistance post-chemotherapy is an established clinical problem, this study provides insight on drug resistance and drug response on a cellular resolution. Our results show that, whilst chemotherapy is an effective way to reduce tumours, suboptimal drug dosages may contribute towards drug resistance and, by extension, tumour reinforcement. Thus, in accordance with Nietzschean philosophy, chemotherapy that does not kill a tumour may indeed make it stronger. Generally we found that drug resistance that presents independently of the drug, and thus may precede chemotherapy, is amplified by high drug dosages. However, drug resistance that is induced by drug presence is accelerated by low to moderate drug dosages. These findings are pictorially demonstrated in Figure 10.

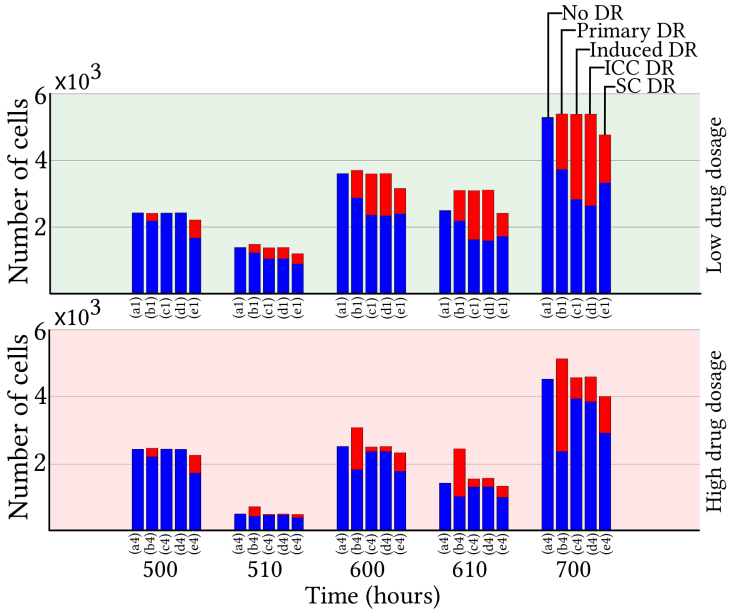

Figure 8: Diagram of the drug sensitive subpopulation (blue) and the drug resistant subpopulation. Various types of drug resistance are incorporated namely (a) No DR, (b) Primary DR, (c) Induced DR, (d) ICC DR, (e) SC DR. Results are shown at times 500 h (immediately before the first drug dose), 510 h, 600 h (immediately before the second drug dose), 610 h and 700 h (end of simulation) for low drug dosages, (1) 1C, and high drug dosages, (4) 8C. Each diagram shows the average value based on 100 simulations.

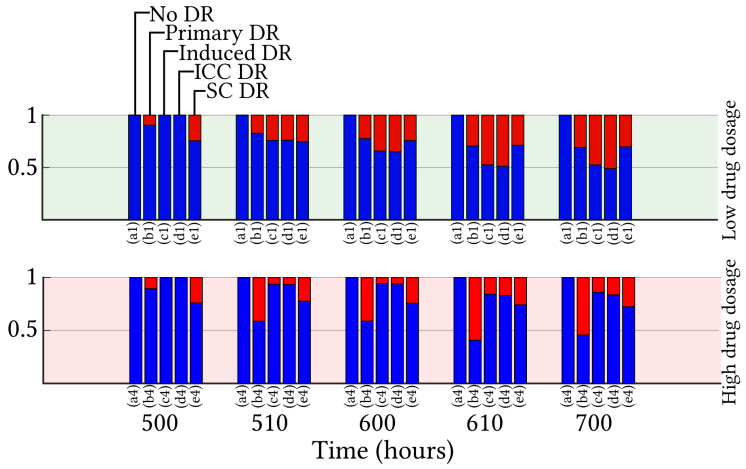

Figure 9: Diagram of the ratio between the drug sensitive subpopulation (blue) and the drug resistant sub-population. Various types of drug resistance are incorporated namely (a) No DR, (b) Primary DR, (c) Induced DR, (d) ICC DR, (e) SC DR. Results are shown at times 500 h (immediately before the first drug dose), 510 h, 600 h (immediately before the second drug dose), 610 h and 700 h (end of simulation) for low drug dosages, (1) 1C, and high drug dosage, (4) 8C. Each diagram shows the average value based on 100 simulations.

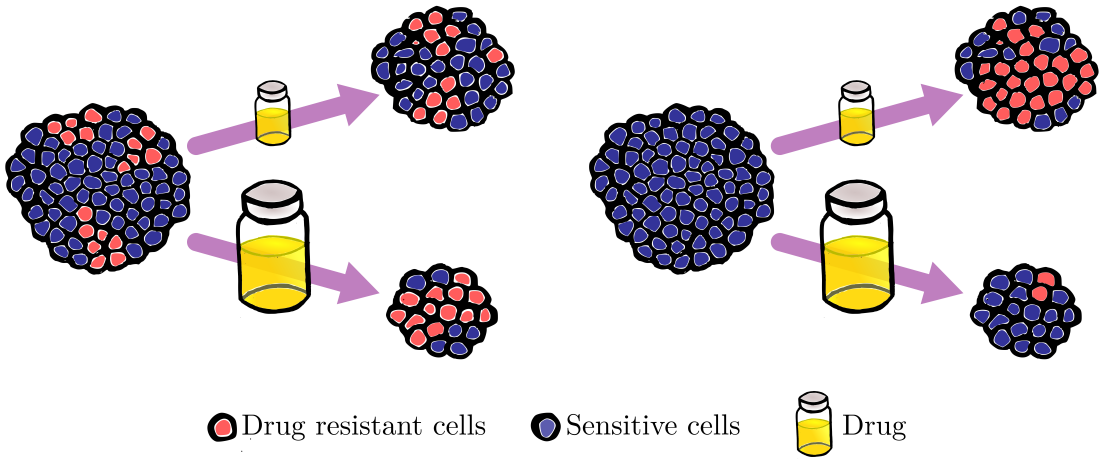

Figure 10: Tumours exposed to chemotherapeutic drugs given in low (top) or high (bottom) dosages, the latter dosage option kills more cancer cells. One of the tumours (left) expresses drug resistance pre chemotherapy, the other one (right) does not. Generally in our *in silico* experiment, drug resistance that occurs independently of the drug, and thus may precede chemotherapy, is amplified by high drug dosages (left). Conversely, drug resistance that is induced by drug presence is accelerated by low to moderate drug dosages (right).

Acknowledgements

SH gratefully acknowledge the support of Swansea University PhD Research Studentship.

References

[1] K. Abubaker, A. Latifi, R. Luwor, S. Nazaretian, H. Zhu, M. A. Quinn, E. W. Thompson, J. K. Findlay, and N. Ahmed. Short-term single treatment of chemotherapy results in the enrichment of ovarian cancer stem cell-like cells leading to an increased tumor burden. *Mol. Cancer*, 12:24, Mar 2013.

[2] J. Adamski, A. Price, C. Dive, and G. Makin. Hypoxia-induced cytotoxic drug resistance in osteosarcoma is independent of HIF-1Alpha. *PLoS ONE*, 8(6):e65304, 2013.

[3] T. Alarcon, H. M. Byrne, and P. K. Maini. A cellular automaton model for tumour growth in inhomogeneous environment. *J. Theor. Biol.*, 225:257–274, Nov 2003.

[4] A. R. Anderson, K. A. Rejniak, P. Gerlee, and V. Quaranta. Microenvironment driven invasion: a multiscale multimodel investigation. *J Math Biol*, 58:579–624, Apr 2009.

[5] Ayachit and Utkarsh. The ParaView Guide: A Parallel Visualization Application, ISBN: 978-1930934306. *Kitware*, 2015.

[6] Nicola Bellomo, NK Li, and Ph K Maini. On the foundations of cancer modelling: selected topics, speculations, and perspectives. *Mathematical Models and Methods in Applied Sciences*, 18(04):593–646, 2008.

[7] G. Cesi, G. Walbrecq, C. Margue, and S. Kreis. Transferring intercellular signals and traits between cancer cells: extracellular vesicles as "homing pigeons". *Cell Commun. Signal*, 14(1):13, Jun 2016.

[8] C. L. Chaffer, I. Brueckmann, C. Scheel, A. J. Kaestli, P. A. Wiggins, L. O. Rodrigues, M. Brooks, F. Reinhardt, Y. Su, K. Polyak, L. M. Arendt, C. Kuperwasser, B. Bierie, and R. A. Weinberg. Normal and neoplastic nonstem cells can spontaneously convert to a stem-like state. *Proc. Natl. Acad. Sci. U.S.A.*, 108(19):7950–7955, May 2011.

[9] K. Chen, W. Cao, J. Li, D. Sprengers, P. Y. Hernanda, X. Kong, L. J. Van Der Laan, K. Man, J. Kwekkeboom, H. J. Metselaar, M. P. Peppelenbosch, and Q. Pan. Differential Sensitivities of Fast- and Slow-cycling Cancer Cells to Inosine Monophosphate Dehydrogenase 2 Inhibition by Mycophenolic Acid. *Mol. Med.*, Oct 2015.

[10] T. S. Deisboeck, Z. Wang, P. Macklin, and V. Cristini. Multiscale cancer modeling. *Annu Rev Biomed Eng*, 13:127–155, Aug 2011.

[11] J. L. Dembinski and S. Krauss. Characterization and functional analysis of a slow cycling stem cell-like subpopulation in pancreas adenocarcinoma. *Clin. Exp. Metastasis*, 26(7):611–623, 2009.

[12] G. Duan, Q. Tang, H. Yan, L. Xie, Y. Wang, X. E. Zheng, Y. Zhuge, S. Shen, B. Zhang, X. Zhang, J. Wang, W. Wang, and X. Zou. A Strategy to Delay the Development of Cisplatin Resistance by Maintaining a Certain Amount of Cisplatin-Sensitive Cells. *Sci Rep*, 7(1):432, Mar 2017.

[13] J. Foo and F. Michor. Evolution of acquired resistance to anti-cancer therapy. *J. Theor. Biol.*, 355:10–20, Aug 2014.

[14] H. B. Frieboes, B. R. Smith, Z. Wang, M. Kotsuma, K. Ito, A. Day, B. Cahill, C. Flinders, S. M. Mumenthaler, P. Mallick, E. Simbawa, A. S. Al-Fhaid, S. R. Mahmoud, S. S. Gambhir, and V. Cristini. Predictive Modeling of Drug Response in Non-Hodgkin's Lymphoma. *PLoS ONE*, 10(6):e0129433, 2015.

[15] P. Gerlee and A. R. Anderson. An evolutionary hybrid cellular automaton model of solid tumour growth. *J. Theor. Biol.*, 246:583–603, Jun 2007.

[16] M. Gerlinger and C. Swanton. How Darwinian models inform therapeutic failure initiated by clonal heterogeneity in cancer medicine. *Br. J. Cancer*, 103(8):1139–1143, Oct 2010.

[17] H. Guo, J. Dong, S. Hu, X. Cai, G. Tang, J. Dou, M. Tian, F. He, Y. Nie, and D. Fan. Biased random walk model for the prioritization of drug resistance associated proteins. *Sci Rep*, 5:10857, Jun 2015.

[18] M. M. Hadjiandreou and G. D. Mitsis. Mathematical modeling of tumor growth, drug-resistance, toxicity, and optimal therapy design. *IEEE Trans Biomed Eng*, 61(2):415–425, Feb 2014.

[19] H. Harashima, N. Dissmeyer, and A. Schnittger. Cell cycle control across the eukaryotic kingdom. *Trends Cell Biol.*, 23(7):345–356, Jul 2013.

[20] Trachette L Jackson and Helen M Byrne. A mathematical model to study the effects of drug resistance and vasculature on the response of solid tumors to chemotherapy. *Mathematical biosciences*, 164(1):17–38, 2000.

[21] A. R. Kansal, S. Torquato, G. R. Harsh IV, E. A. Chiocca, and T. S. Deisboeck. Cellular automaton of idealized brain tumor growth dynamics. *BioSystems*, 55:119–127, Feb 2000.

[22] Z. Kozovska, V. Gabrisova, and L. Kucerova. Colon cancer: cancer stem cells markers, drug resistance and treatment. *Biomed. Pharmacother.*, 68(8):911–916, Oct 2014.

[23] K. R. Kutanzi, O. V. Yurchenko, F. A. Beland, V. F. Checkhun, and I. P. Pogribny. MicroRNA-mediated drug resistance in breast cancer. *Clin Epigenetics*, 2(2):171–185, Aug 2011.

[24] O. Lavi, M. M. Gottesman, and D. Levy. The dynamics of drug resistance: a mathematical perspective. *Drug Resist. Updat.*, 15(1-2):90–97, 2012.

[25] A. Lorz, D. A. Botesteanu, and D. Levy. Modeling Cancer Cell Growth Dynamics In vitro in Response to Antimitotic Drug Treatment. *Front Oncol*, 7:189, 2017.

[26] S. E. Luria and M. Delbruck. Mutations of Bacteria from Virus Sensitivity to Virus Resistance. *Genetics*, 28(6):491–511, Nov 1943.

[27] P. Macklin, S. McDougall, A. R. A. Anderson, M. A. J. Chaplain, V. Cristini, and J. Lowengrub. Multiscale modelling and nonlinear simulation of vascular tumour growth. *J Math Biol*, 58:765–798, Apr 2009.

[28] H. C. Monro and E. A. Gaffney. Modelling chemotherapy resistance in palliation and failed cure. *J. Theor. Biol.*, 257(2):292–302, Mar 2009.

[29] N. Moore, J. Houghton, and S. Lyle. Slow-cycling therapy-resistant cancer cells. *Stem Cells Dev.*, 21(10):1822–1830, Jul 2012.

[30] C. Munck, H. K. Gumpert, A. I. Wallin, H. H. Wang, and M. O. Sommer. Prediction of resistance development against drug combinations by collateral responses to component drugs. *Sci Transl Med*, 6(262):262ra156, Nov 2014.

[31] E. L. Niero, B. Rocha-Sales, C. Lauand, B. A. Cortez, M. M. de Souza, P. Rezende-Teixeira, M. S. Urabayashi, A. A. Martens, J. H. Neves, and G. M. Machado-Santelli. The multiple facets of drug resistance: one history, different approaches. *J. Exp. Clin. Cancer Res.*, 33:37, Apr 2014.

[32] M. R. Owen, T. Alarcon, P. K. Maini, and H. M. Byrne. Angiogenesis and vascular remodelling in normal and cancerous tissues. *J Math Biol*, 58:689–721, Apr 2009.

[33] John Carl Panetta. A mathematical model of periodically pulsed chemotherapy: tumor recurrence and metastasis in a competitive environment. *Bulletin of mathematical Biology*, 58(3):425–447, 1996.

[34] A. W. Park, J. Haven, R. Kaplan, and S. Gandon. Refugia and the evolutionary epidemiology of drug resistance. *Biol. Lett.*, 11(11), Nov 2015.

[35] A. A. Patel, E. T. Gawlinski, S. K. Lemieux, and R. A. Gatenby. A cellular automaton model of early tumor growth and invasion. *J. Theor. Biol.*, 213:315–331, Dec 2001.

[36] J. Perez-Velazquez, J. L. Gevertz, A. Karolak, and K. A. Rejniak. Microenvironmental Niches and Sanctuaries: A Route to Acquired Resistance. *Adv. Exp. Med. Biol.*, 936:149–164, 2016.

[37] H. Perfahl, H. M. Byrne, T. Chen, V. Estrella, T. Alarcon, A. Lapin, R. A. Gatenby, R. J. Gillies, M. C. Lloyd, P. K. Maini, M. Reuss, and M. R. Owen. Multiscale modelling of vascular tumour growth in 3D: the roles of domain size and boundary conditions. *PLoS ONE*, 6:e14790, 2011.

[38] G. G. Powathil, D. J. Adamson, and M. A. Chaplain. Towards predicting the response of a solid tumour to chemotherapy and radiotherapy treatments: clinical insights from a computational model. *PLoS Comput. Biol.*, 9(7):e1003120, Jul 2013.

[39] G. G. Powathil, K. E. Gordon, L. A. Hill, and M. A. Chaplain. Modelling the effects of cell-cycle heterogeneity on the response of a solid tumour to chemotherapy: biological insights from a hybrid multiscale cellular automaton model. *J. Theor. Biol.*, 308:1–19, Sep 2012.

[40] G. G. Powathil, M. Swat, and M. A. Chaplain. Systems oncology: towards patient-specific treatment regimes informed by multiscale mathematical modelling. *Semin. Cancer Biol.*, 30:13–20, Feb 2015.

[41] Gibin G Powathil, Mark AJ Chaplain, and Maciej Swat. Investigating the development of chemotherapeutic drug resistance in cancer: A multiscale computational study. *arXiv preprint arXiv:1407.0865*, 2014.

[42] P. A. Reece, I. Stafford, M. Davy, and S. Freeman. Disposition of unchanged cisplatin in patients with ovarian cancer. *Clin. Pharmacol. Ther.*, 42(3):320–325, Sep 1987.

[43] B.T. Ribba, T. Alarcon, K. Marron, P.K Maini, and Z Agur. The Use of Hybrid Cellular Automaton Models for Improving Cancer Therapy. *Lect. notes comput. sci*, 3305:444–453, 2004.

[44] S. Rizzo, J. M. Hersey, P. Mellor, W. Dai, A. Santos-Silva, D. Liber, L. Luk, I. Titley, C. P. Carden, G. Box, D. L. Hudson, S. B. Kaye, and R. Brown. Ovarian cancer stem cell-like side populations are enriched following chemotherapy and overexpress EZH2. *Mol. Cancer Ther.*, 10(2):325–335, Feb 2011.

[45] A. Roberti, D. La Sala, and C. Cinti. Multiple genetic and epigenetic interacting mechanisms contribute to clonally selection of drug-resistant tumors: current views and new therapeutic prospective. *J. Cell. Physiol.*, 207(3):571–581, Jun 2006.

[46] Tiina Roose, S Jonathan Chapman, and Philip K Maini. Mathematical models of avascular tumor growth. *Siam Review*, 49(2):179–208, 2007.

[47] S. Rottenberg and P. Borst. Drug resistance in the mouse cancer clinic. *Drug Resist. Updat.*, 15(1-2):81–89, 2012.

[48] N. A. Saunders, F. Simpson, E. W. Thompson, M. M. Hill, L. Endo-Munoz, G. Leggatt, R. F. Minchin, and A. Guminski. Role of intratumoural heterogeneity in cancer drug resistance: molecular and clinical perspectives. *EMBO Mol Med*, 4(8):675–684, Aug 2012.

[49] S. Srinivasan, F. O. Vannberg, and J. B. Dixon. Lymphatic transport of exosomes as a rapid route of information dissemination to the lymph node. *Sci Rep*, 6:24436, Apr 2016.

[50] T. Srinivasan, J. Walters, P. Bu, E. B. Than, K. L. Tung, K. Y. Chen, N. Panarelli, J. Milsom, L. Augenlicht, S. M. Lipkin, and X. Shen. NOTCH Signaling Regulates Asymmetric Cell Fate of Fast- and Slow-Cycling Colon Cancer-Initiating Cells. *Cancer Res.*, 76(11):3411–3421, Jun 2016.

[51] A Stéphanou and Vitaly Volpert. Hybrid modelling in biology: a classification review. *Mathematical Modelling of Natural Phenomena*, 11(1):37–48, 2016.

[52] X. Sun, J. Bao, and Y. Shao. Mathematical Modeling of Therapy-induced Cancer Drug Resistance: Connecting Cancer Mechanisms to Population Survival Rates. *Sci Rep*, 6:22498, Mar 2016.

[53] D. P. Tabassum and K. Polyak. Tumorigenesis: it takes a village. *Nat. Rev. Cancer*, 15(8):473–483, Aug 2015.

[54] M. Tong, W. Zheng, X. Lu, L. Ao, X. Li, Q. Guan, H. Cai, M. Li, H. Yan, Y. Guo, P. Chi, and Z. Guo. Identifying clinically relevant drug resistance genes in drug-induced resistant cancer cell lines and post-chemotherapy tissues. *Oncotarget*, 6(38):41216–41227, Dec 2015.

[55] G. Tzedakis, E. Liapis, E. Tzamali, G. Zacharakis, and V. Sakkalis. A hybrid discrete-continuous model of in vitro spheroid tumor growth and drug response. *Conf Proc IEEE Eng Med Biol Soc*, 2016:6142–6145, Aug 2016.

[56] F. Un. G1 arrest induction represents a critical determinant for cisplatin cytotoxicity in G1 checkpoint-retaining human cancers. *Anticancer Drugs*, 18(4):411–417, Apr 2007.

[57] A. Wu, K. Loutherback, G. Lambert, L. Estevez-Salmeron, T. D. Tlsty, R. H. Austin, and J. C. Sturm. Cell motility and drug gradients in the emergence of resistance to chemotherapy. *Proc. Natl. Acad. Sci. U.S.A.*, 110(40):16103–16108, Oct 2013.

[58] L. Zhang, Z. Wang, J. A. Sagotsky, and T. S. Deisboeck. Multiscale agent-based cancer modeling. *J Math Biol*, 58(4-5):545–559, Apr 2009.

[59] X. Zhang, X. Yuan, H. Shi, L. Wu, H. Qian, and W. Xu. Exosomes in cancer: small particle, big player. *J Hematol Oncol*, 8:83, Jul 2015.

Supplementary Material

What does not kill a tumour may make it stronger: *in silico* Insights on Chemotherapeutic Drug Resistance

Sara Hamis[1,2], Perumal Nithiarasu[3], Gibin G Powathil[1,2]

[1] Department of Mathematics, College of Science, Swansea University, Swansea, SA2 0JB.
[2] Computational Foundry, Swansea University, Swansea, SA1 8EN.

5 Intracellular and Extracellular Dynamics

5.1 Parameters involved in regulating the cell cycle

This section contains parameters occurring in Section 2.1.1, Equation 1 in the original paper. Parameters are gathered from Powathil et al. 2012 [39] and correspond to cell-cycle lengths averaging 25 hours.

Component	Rate constants (h^{-1})	Dimensionless constants
[CycB]	$k_1 = 0.12$, $k_2' = 0.12$	
	$k_2'' = 4.5$, [p27/p21]$= 1.05$	
[Cdh1]	$k_3' = 3$, $k_3'' = 30$, $k_4 = 105$	$J_3 = 0.04$, $J_4 = 0.04$
[p55cdc$_T$]	$k_5' = 0.015$, $k_5'' = 0.6$, $k_6 = 0.3$	$J_5 = 0.3$, $n = 4$
[p55cdc$_A$]	$k_7 = 3$, $k_8 = 1.5$	$J_7 = 0.001$, $J_8 = 0.001$, [Mad]$= 1$
[Plk1]	$k_9 = 0.3$, $k_{10} = 0.06$	
[mass]	$\mu = \mu^+ + \epsilon\hat{\mu}$, $\mu^+ = 0.03$	$m_* = 10$, ϵ is randomised, $\epsilon \in [-1, 1]$

Table 2: Parameters for Equation 1.

$$[HIF1] = \begin{cases} 1 & \text{if } K \leq 0.1 \\ 0 & \text{otherwise} \end{cases}$$

5.2 Parameters for oxygen and drug distribution

This section contains parameters occurring in Section 2.1.2, Equations 2 and 3, in the original paper.

Parameter	Symbol	Value	Reference
Oxygen diffusion coefficient	D_k	$2.5 \cdot 10^{-5}$ [cm$^2 s^{-1}$]	[39]
Oxygen supply rate	r_k	$8.2 \cdot 10^{-3}[s^{-1}]$	[39]
Oxygen consumption rate	ϕ_k	$2 \cdot 10^{-1}$ [s^{-1}]	[39]
Cisplatin diffusion coefficient	D_c	$7.6 \cdot 10^{-6}$ [cm$^2 s^{-1}$]	[39]
Cisplatin supply rate	r_c	*estimated*	
Cisplatin consumption rate	ϕ_c	0 *(negligable)*	[39]
Cisplatin decay rate	η_c	*estimated*	[42]

Table 3: Parameters for Equations 2 and 3.

Diffusion and production rates of oxygen and drugs vary across the grid so that [39]

$$D_i(x,t) = \begin{cases} \frac{D_i}{1.5} & \text{in the tumour,} \\ D_i & \text{elsewhere,} \end{cases}$$

for $i = k, c$ and

$$r_k(x,t) = \begin{cases} \frac{r_k}{1.5} & \text{in the tumour,} \\ r_k & \text{elsewhere,} \end{cases} \qquad r_c(x,t) = \begin{cases} \frac{r_c}{1.5} & \text{in the tumour,} \\ r_c & \text{on the tumour boundary,} \\ \frac{r_c}{2} & \text{outside tumour.} \end{cases}$$

The drug decay rate η_c is estimated to match the half-life time of cisplatin which has been reported as 31.6 ± 6 minutes [42]. The cisplatin supply rate r_c is 0 at times when drugs are not administrated and at times of drug administration r_c is scaled according to the drug dosage so that

$$p \cdot \mathrm{C} = r_c \cdot (\text{number of blood vessels}),$$

hence r_c corresponds to the amount of drug produced at one blood vessel cross section at one time step. Here $p = 1, 2, 4, 8$ in accordance with the possible drug dosages in the *in silico* experiment which are 1C, 2C, 4C and 8C. A cell in location x at time t is killed if the drug concentration is such that $\mathscr{C}(x,t) \geq \kappa$. C and κ are parametrised so that 1C kills half of the cell population in absence of any drug resistance. Specifically we here chose C= 10^4 (equal to the number of grid points) and $\kappa = 0.18$. Since C is equal to the number of grid points, all cancer cells would die immediately from drug exposure if drugs were produced homogeneously across the grid, as such a scenario would yield a drug concentration $\mathscr{C}(x,t) = 1 > \kappa \ \ \forall x$.

6 Drug Resistance

This section contains parameters and algorithms used in Sections 2.2.1 through to 2.2.4 in the original paper. The chosen parameter values for the *in silico* framework are listed in Table 4,

α_{pri}	χ_{ind}	τ	α_{ex}	α_{SC}
0.01	$\kappa/10$	30 minutes	0.07	0.07

Table 4: Parameters concerning drug resistance used in the *in silico* framework.

where in hypoxic regions α_{ex} is increased to $2\alpha_{ex}$.

6.1 Model

This section demonstrates partial algorithms which are used to compute if a cell is drug resistant or not.

6.1.1 Primary drug resistance

Each time cell division occurs there is a chance that a drug resistant cell will be produced. In the model, when cell division occurs we say that a mother cell produces a daughter cell. If the mother cell is drug resistant (DR), there daughter cell will inherently be drug resistant. However, if the mother cell is sensitive (S), the daughter cell may or may not be drug resistant. At each cell division a value $\alpha \in [0, 1]$ is randomised, if $\alpha \leq \alpha_{pri}$ then the daughter cell is drug resistant, otherwise it is sensitive, as schematically shown in Figure 6.1.1.

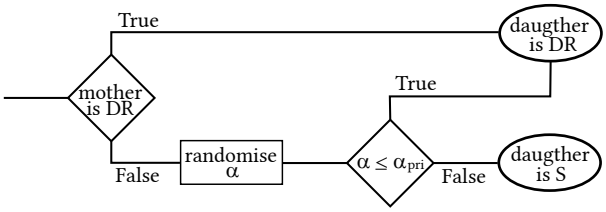

Figure 11: Partial algorithm for determining primary drug resistance.

6.1.2 Induced drug resistance

If a cell has experienced a minimum drug concentration χ_{ind} for τ time units, drug resistance is induced in the cell. Thus in the model we use a counter, counter_n, individual to each cell, that increments each time step that cell_n experiences a drug concentration $\chi = \mathscr{C}(x,t) \geq \chi_{ind}$. This is schematically illustrated in Figure 6.1.2. If drug resistance has been produced in a mother cell it produces drug resistant daughter cells.

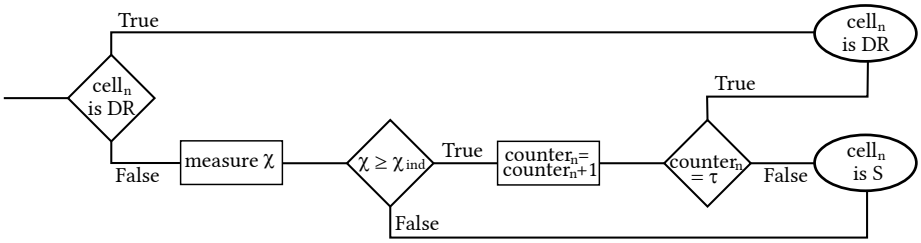

Figure 12: Partial algorithm for determining induced drug resistance.

6.1.3 Communicated drug resistance via exosomes

Once per cell cycle, each cell that has acquired induced drug resistance (see above section) or communicated drug resistance (as described in this section) has a chance α_{ex} of producing and secreting an exosome. In the model, a value $\alpha \in [0,1]$ is randomised, if $\alpha \leq 2\alpha_{ex}$ in hypoxic regions, or $\alpha \leq \alpha_{ex}$ in normoxic or hyperoxic regions, an exosome is produced an sent off in a random direction. The first sensitive cell that the exosome hits becomes drug resistant, as schematically shown in Figure 6.1.3.
[h]

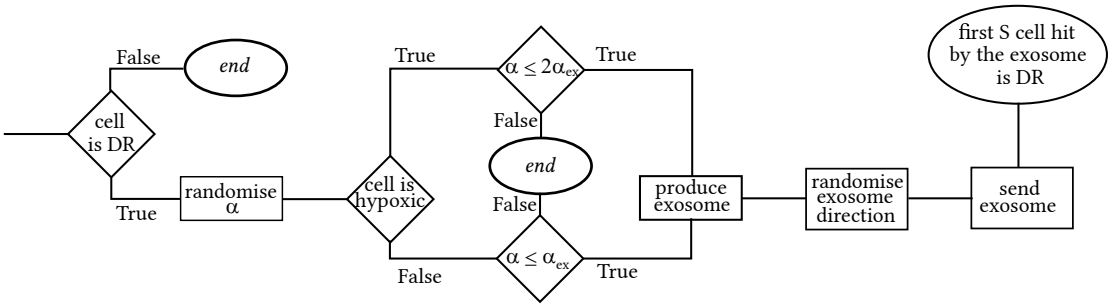

Figure 13: Partial algorithm for determining exosome production.

6.1.4 Cell cycle mediated drug resistance by slow-cycling cells

Once per cell-cycle there is a chance that a sensitive, fast-cycling (FC) cell will spontaneously convert to a slow-cycling (SC), drug resistant state. A value $\alpha \in [0, 1]$ is randomised, if $\alpha \leq \alpha_{SC}$ then the cell converts, otherwise it does not, as demonstrated in Figure 6.1.4.

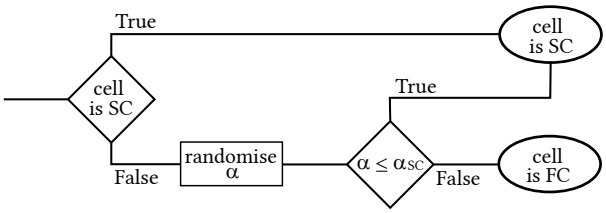

Figure 14: Partial algorithm for determining the spontaneous convertion from a slow-cycling to a fast-cycling state.

7 Sensitivity analysis

To verify that our results are robust in regards to the chosen parameters listed in Table 4, a sensitivity analysis is preformed in which we vary these parameters accoring to Table 5. Each sensitivity test is run 100 times, results are provided in Figure 7. These results show that our qualitative findings, concerning drug response in cancer cell populations hosting various types of drug resistance, hold for parameter variations. Indeed the ratio of drug resistant cells increases with high drug dosages in cases where drug resistance precedes chemotherapy, here in experiments (b) Primary DR and (e) Cell cycle mediated drug resistance by spontaneous conversion to slow-cycling cells. Conversely drug-induced drug resistance is amplified in low drug dosages, here in experiments (c) Induced DR and (d) Induced and, via exosomes, communicated drug resistance.

Experiment	Parameter	original test	sensitivity test 1	sensitivity test 2	sensitivity test 3	sensitivity test 4
b	α_{pri}	0.01	0.005	0.025		
c	χ_{ind}	$\kappa/5$	$\kappa/5$	$\kappa/5$	$\kappa/10$	$\kappa/2$
c	τ[minutes]	30	15	60	30	30
d	α_{ex}	0.05	0.03	0.1		
d	χ_{ind}	$\kappa/5$	$\kappa/5$	$\kappa/5$		
d	τ[minutes]	30	30	30		
e	α_{SC}	0.07	0.03	0.1		

Table 5: Parameters used in testing the robustness of the model.

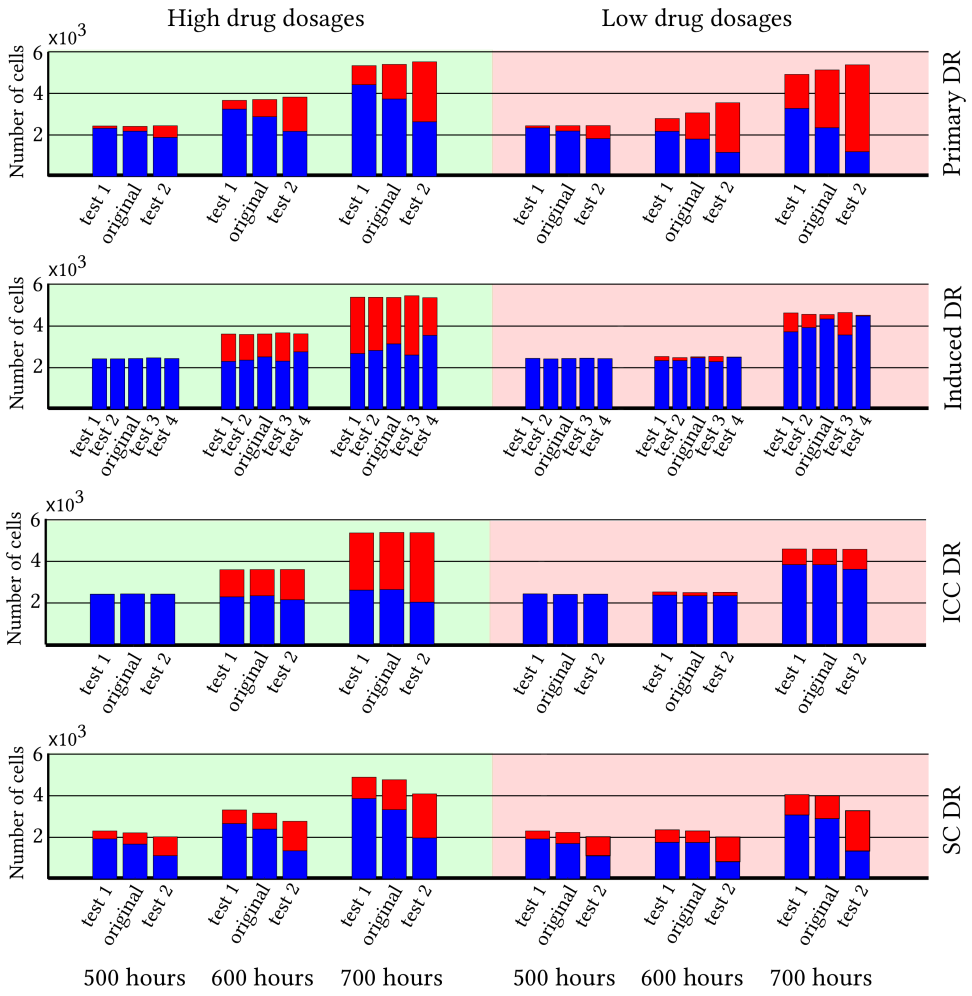

Figure 15: Sensitivity analysis, showing the number of sensitive (blue) and drug resistant (red) cells at three time points when low (left) and high (right) drug dosages are administered, namely 1C and 8C respectively. Each test is performed 100 times and the parameters for each test are listed in Table 5.